Corrosion Science 87 (2014) 376–382

Contents lists available at ScienceDirect

Corrosion Science

journal homepage: www.elsevier.com/locate/corsci

Application of automated electrical resistance sensors for measurement of corrosion rate of copper, bronze and iron in model indoor atmospheres containing short-chain volatile carboxylic acids

Tomas Prosek [a,*], Michelle Taube [b], Francois Dubois [a], Dominique Thierry [a]

[a] Institut de la Corrosion/French Corrosion Institute, 220 rue Pierre Rivoalon, 29200 Brest, France
[b] The National Museum of Denmark, Dept. of Conservation and Natural Sciences, Brede, Denmark

ARTICLE INFO

Article history:
Received 27 February 2014
Accepted 14 June 2014
Available online 25 June 2014

Keywords:
A. Copper
A. Bronze
A. Iron
C. Atmospheric corrosion

ABSTRACT

The corrosion rate of copper and bronze Cu-8 wt.%Sn increased rapidly when the concentration of formic or acetic acid in air reached about 300 ppb at 80% relative humidity (RH) and a temperature of 20 °C. It decreased slowly during the several days after pollutant removal due to the slow rate of pollutant desorption from the metal surfaces. Corrosion of these metals was barely affected by the acids at RH up to 60%. For iron, the critical concentration of formic acid in air which led to surface activation at 80% RH was between 1000 and 1590 ppb.

1. Introduction

Formic acid, HCOOH, and acetic acid, CH_3COOH, are major corrosive pollutants in indoor cultural heritage premises. In contrast to sulphur dioxide, nitrogen dioxide and ozone, which come from external sources, they are of internal origin emitted primarily by wooden furniture [1–6]. Aside from the wood itself, carboxylic acids are released from the glues, adhesives, varnish and plastic accessories used regularly by the furniture industry [2,7]. Hardwoods, e.g. oak, beech and mahogany, are known to emit more acetic acid than softwoods due to a higher content of hemicellulose with acetyl group esters, which are prone to hydrolyse to acetic acid [3]. The emission of formic acid from wood is generally an order of magnitude lower than that of acetic acid, but still not negligible [3]. Other sources of carboxylic acids in museums and archives are hemicellulose-containing wrapping papers and cardboards [4], exhibited or stored objects made of wood, paper and some plastics [4,5], and conservation and preparation materials [7]. Smaller amounts of these pollutants may come from biogenic sources [1] and decomposition reactions, e.g., formaldehyde may decompose to formic acid upon adsorption on surfaces [2,7] and isoprene can be photo-oxidized to formic acid [8].

Typical concentrations of acetic acid in clean, low troposphere and urban areas are 0.1–2 and 0.2–8 ppb, respectively [9]. Due to the numerous indoor sources of short-chain volatile carboxylic acids, their concentrations in rooms, showcases, storage facilities and cabinets usually exceed background outdoor levels. In indoor residences, concentrations of formic acid range from 9 to 33 ppb while those of acetic acid range from 9 to 88 ppb [10]. Allen and Miguel reported that exposure to acetic acid was enhanced 2–15 times indoors at different Brazilian sites [1]. Concentrations in hundreds or even thousands of ppb have repeatedly been reported in enclosures with limited air exchange in cultural heritage institutions [1,3,5,7,11–13]. When extreme values are excluded, concentrations of formic and acetic acid in indoor museum atmospheres range from low levels up to 500 and 2000 ppb, respectively.

Short-chain volatile carboxylic acids were reported to accelerate the degradation of objects made of lead [2–6], bronze and copper [3,5], zinc [4], iron [3], and glass [3] and to cause efflorescence on calcareous materials, such as shells, fossils, ceramics, pottery and limestone [3–5]. The deterioration of other materials such as paper or plastics can also be accelerated in their presence due to acidification [5]. Based on previous studies, recommendations on maximal concentrations of formic and acetic acids in indoor atmospheres were issued. The maximum average concentration of acetic acid for a 1- and 100-year preservation target for museum, gallery, library, and archival collections is set to 400 and 40 ppb, respectively, by the ASHRAE Handbook [9]. However, lower limits may be necessary for particularly sensitive materials such as lead.

Concentrations of short-chain volatile carboxylic acids in air can be measured using active or passive sampling techniques [5,11].

* Corresponding author. Tel.: +33 298 058 905; fax: +33 298 050 894.
E-mail address: tomas.prosek@institut-corrosion.fr (T. Prosek).

http://dx.doi.org/10.1016/j.corsci.2014.06.047
0010-938X/

Passive sampling is more affordable; however, the results of an assessment are typically available only after a delay of several months following exposure of the samplers, transport and analysis in a specialized laboratory. In addition, the impact of carboxylic acids on material degradation is affected by a complex interplay among numerous factors such as temperature, relative humidity, the presence of other pollutants and ventilation patterns, which have not been fully investigated yet. Thus, it may be preferable to monitor their direct impact on materials of interest. This is traditionally done by exposing coupons of given materials to the environment and analysing their degradation after a certain exposure period. According to current standards and recommendations, a metal coupon needs to be exposed for 30 days or for 1 year [14–16]. The impact of the environment on metal degradation is then evaluated based on mass loss, mass gain or coulometric reduction of the corrosion products. The mass loss procedure is used for an assessment of outdoor corrosivity whereas mass gain is usually measured on coupons exposed indoors. The coulometric reduction of corrosion products is more demanding with respect to equipment and expertise but can provide an indication of the nature of the pollution in addition to the rate of metal degradation.

However, none of these techniques yields real-time data. Within the exposure period, valuable objects might further deteriorate if the air is contaminated. Since it is believed that information on the present corrosivity of the atmosphere is crucial to effective corrosion protection, an electronic logger, called AirCorr, which allows for continuous measurement of the corrosion rate of a metal in air has been developed [17,18]. The logger provides very high sensitivity enabling real-time corrosion monitoring even in low-corrosivity indoor facilities, good reproducibility for metals corroding mostly uniformly in a given environment, and good accuracy [19–23]. It makes use of the electrical resistance (ER) technique to monitor corrosivity. The use of ER is described in, e.g., ASTM standard G96 [24]. The concept is simple and yet highly effective: the electronic unit measures and registers the change over time of the electrical resistance of a thin metal track applied on an insulating substrate. If the metal corrodes, the cross-sectional area of the track decreases and the electrical resistance increases. A part of the metal track is protected by an organic coating or tape and, thus, serves as a reference to compensate for resistivity changes due to temperature variations. Based on the initial cross-sectional area of the exposed element, the cumulative metal loss at the time of reading can be determined.

For a metal film with constant thickness corroding uniformly, the extent of corrosion can be represented as a corrosion depth. Assuming that the electrical conductivity of the track is proportional to the remaining metal track thickness and assuming that corrosion products do not contribute to the conductivity, the corrosion depth of the metallic sensor, Δh, can be calculated according to the equation

$$\Delta h = h_{\mathrm{ref,init}}\left(\frac{R_{\mathrm{ref,init}}}{R_{\mathrm{sens,init}}} - \frac{R_{\mathrm{ref}}}{R_{\mathrm{sens}}}\right) \quad (1)$$

where $h_{\mathrm{ref,init}}$ is the initial thickness of the reference metallic track, which is assumed equal to the sensor track at the beginning of exposure; R_{sens} and R_{ref} are the current resistances of the sensor and reference tracks; and $R_{\mathrm{sens,init}}$ and $R_{\mathrm{ref,init}}$ are the initial resistances of the sensor and reference tracks [20]. The calculation is based on the electrical resistance measured as a potential difference along the track through which a defined current passes.

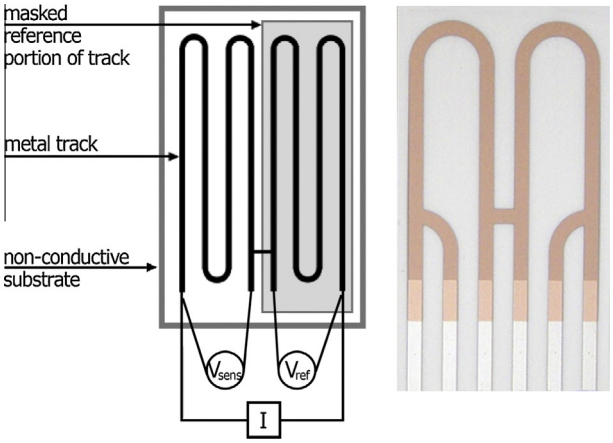

Fig. 1. Electrical resistance corrosion sensor; schematic drawing (left) and photograph of a 500-nm copper sensor (right).

Sensors made of the most technically important and some historical metal alloys in different thicknesses and sensitivities have also been developed [19,25]. A schematic drawing of a sensor is shown in Fig. 1 along with a photograph of one of the sensors without the reference part protection. The metal tracks were laid down by magnetron sputtering on a fine-grained Al_2O_3 ceramic substrate [21]. The width of the measuring track is from 1 to 2 mm, depending on sensor type, and the length over 100 mm. This geometry ensures high sensitivity to changes in the electrical resistance due to metal corrosion.

For this study, the logger-sensor system was applied to monitor corrosion of copper, bronze and iron in model atmospheres containing controlled concentrations of formic and acetic acid at defined relative humidity and constant temperature. These systems have been studied by other researchers to determine the mechanism and kinetics of corrosion product formation on bulk metal [26–29]. For the thin-film copper, bronze, and iron sensors used in this study, the minimum detectable change in a metal track thickness due to corrosion was below 0.1 nm [19,20]. The main purpose of the work was to confirm the capability of the technique to assess small changes in air corrosivity in real time.

2. Experimental

2.1. Experimental chamber

A chamber allowing for corrosion studies in air with small and well-controlled concentrations of gaseous pollutants was built. It consists of an air dehumidifier, air filter, gas generator, humidifier, exposure chamber and exhaust air treatment unit. A schematic drawing of the system is shown in Fig. 2.

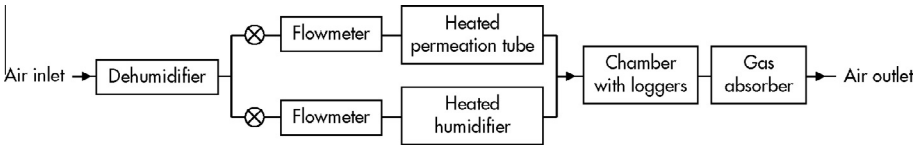

Fig. 2. Experimental setup for corrosion measurements in air polluted with carboxylic acids.

The gas generator used to produce the target pollutant level is made up of an oven with a precisely controlled temperature of between 30 and 100 °C (±0.1 °C) and an air flow controller. A PTFE permeation tube filled with the pollutant of interest is placed into the oven. The permeation rate of a tube depends on the temperature. Calibrated permeation tubes were able to provide up to 1500 ppb of acetic acid or up to 3000 ppb of formic acid in the outlet air.

Part of the feed air was passed through a bottle of demineralised water for humidification before mixing with the stream of polluted air. The polluted, humidified air then entered the exposure chamber that held the loggers.

3. Experimental procedure

Thin-film copper sensors with track thicknesses of 85 and 500 nm (Cu-85 nm, Cu-500 nm), bronze sensors made of Cu-8 wt.%Sn with a thickness of 500 nm (CuSn8–500 nm), and iron sensors with a thickness of 800 nm (Fe-800 nm) were used. The sensors were cleaned with ethanol, dried in a stream of unheated air and inserted into the electronic loggers. The loggers were calibrated after 30 min of temperature stabilisation and moved to the exposure chamber. The loggers were programmed to measure corrosion depth every 15 min.

The temperature and RH in the chamber were measured continuously. The temperature was kept constant at 20 ± 1 °C during the experiment. The relative humidity was controlled to a precision of ±2%. It was measured directly in the chamber and regulated by adjusting the proportion of air passing through the humidifier. The air flow was set to 5 L/min ensuring complete exchange of the air in the chamber within 15 min.

4. Results and discussion

4.1. Corrosivity monitoring

4.1.1. Bronze

Three loggers fitted with CuSn8–500 nm sensors were exposed to air with relative humidity from 15% to 80% RH and formic acid concentration from 0 to 600 ppb. The corrosion depth records are plotted in Fig. 3. The corrosion rates measured by each logger-sensor system are nearly identical. It is evident that both relative humidity and formic acid concentration affect the bronze corrosion rate. The corrosion depth started to increase rapidly after the introduction of the pollutant demonstrating the rapid response of the setup. To the contrary, the corrosion rate decreased only slowly after a decrease in the pollutant concentration. For example, when formic acid stopped being fed into the chamber on Day 2, the corrosion rate dropped but had not fully stabilized even after 3 days. Since the air in the chamber was exchanged every 15 min, this seems to indicate that a film of the adsorbed pollutant was present on the metal surface long after the pollutant was removed from the air. It has been shown that acetate in corrosion products on bronze can be converted to carbonate in the presence of water and carbon dioxide which creates acetic acid for further corrosion reactions [30]. Such a mechanism can be expected to work in presence of formic acid as well.

A similar experiment was carried out in presence of acetic acid. In this case, six parallel CuSn8–500 nm sensors were deployed. An example of a corrosion depth vs. time curve is seen in Fig. 4. It again shows a short response time to increasing air corrosivity. It is interesting to note that a delay of several days was observed before the corrosion rate dropped after the removal of acetic acid from the air even at the very low relative humidity of 15% (see the transition 870 ppb – 80% RH to 0 ppb – 15% RH).

The corrosion rates of bronze, given in Table 1, were obtained from stabilized parts of the curves measured in both environments. Measurements too short to lead to stabilisation and initial measurements were not considered. It must be stressed that stable exposure conditions were maintained for only a few days and the values does not represent long-term corrosion rates.

Based on the current data, the initial aggressiveness of formic acid towards bronze seems to be comparable to that of acetic acid. Qiu and Leygraf found that formic acid is more corrosive than acetic acid on Cu–20Zn brass exposed in air at 90% RH, 20 °C and 120 ppb of the pollutants [29]. In experiments with copper and Cu–Sn–Pb and Cu–Sn–Pb–Zn alloys in air at 100% RH, 30 °C and up to 300 ppb of different carboxylic acids, Bastidas et al. found acetic acid to be usually more corrosive than formic acid [31,32]. However, the relative corrosion rates of the studied bronzes depended strongly on the patina formed and there were cases where formic acid caused higher corrosion rates than acetic acid [31].

The presence of either of the carboxylic acids strongly affected the corrosion rate of bronze at elevated RH whereas it was of limited influence at humidities up to 55% RH. The effect of increasing RH in clean air was also limited below this level.

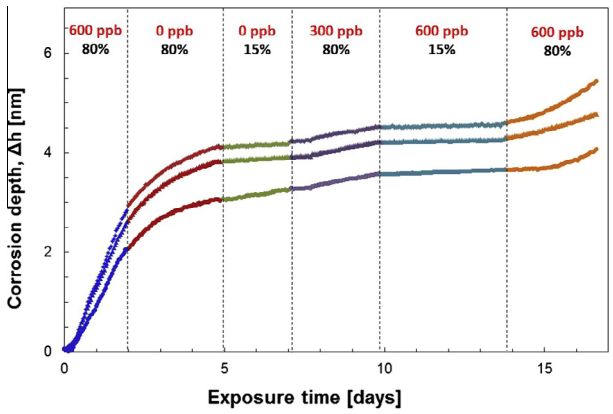

Fig. 3. Corrosion depth measurements on parallel CuSn8–500 nm sensors in air with controlled concentrations of formic acid at 20 °C; numbers give the concentration of formic acid and relative humidity.

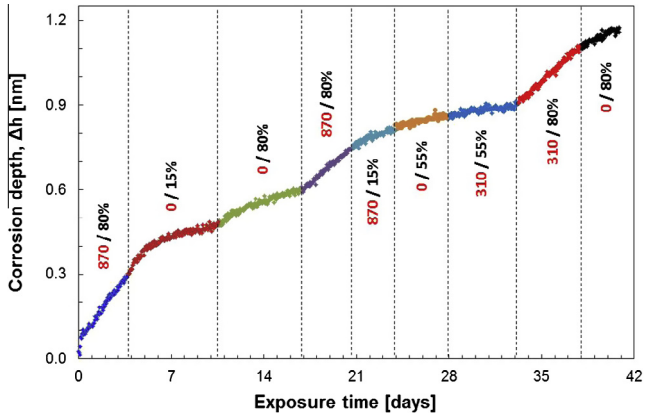

Fig. 4. Corrosion depth records of a CuSn8–500 nm sensor in air with controlled concentrations of acetic acid at 20 °C; numbers give the concentration of acetic acid in ppb and relative humidity in per cent.

Table 1
Corrosion rate of bronze sensors after stabilisation.

Relative humidity, RH (%)	c(HCOOH) (ppb)	c(CH_3COOH) (ppb)	Corrosion rate, v_{corr} (nm/day)	
			Measured	Calculated from Eq. (3)
15	0	0	0.015 ± 0.000	0.003
55	0	0	0.014 ± 0.005	0.011
80	0	0	0.027 ± 0.009	0.016
55	0	310	0.010 ± 0.003	–
80	0	310	0.088 ± 0.017	–
15	0	870	0.022 ± 0.004	–
80	0	870	0.108 ± 0.022	–
80	300	0	0.048 ± 0.007	0.050
15	600	0	0.013 ± 0.000	0.016
80	600	0	0.300 ± 0.057	0.083

A simple empirical model of the effect of carboxylic acids and relative humidity on the corrosion rate can be proposed. The corrosion rate can be expressed as

$$v_{corr} = RH\ (k_1 + k_2\ c) \quad (2)$$

where c is the concentration of carboxylic acid in ppb, RH is relative humidity in % and k_1 and k_2 are constants. For bronze exposed to air containing acetic acid, the corrosion rate in nm/day can thus be expressed as

$$v_{corr} = RH\ \left(2.5 \cdot 10^{-4} + 1.7 \cdot 10^{-6} \cdot c(CH_3COOH)\right) \quad (3)$$

Calculated corrosion rates are compared with experimental data in Table 1.

4.1.2. Copper

Two experiments were performed in which the relative humidity was kept constant during a major part of the exposure and only the formic acid concentration was varied. Three Cu-500 nm and three Cu-85 nm sensors were exposed to air at 80% and 60% RH, respectively, with increasing acid concentrations. It should be noted that due to the use of different permeation tubes with formic acid, the concentrations were slightly different in the two experiments.

An example of the corrosion depth record for a Cu-500 nm sensor is plotted in Fig. 5. The other records were similar. The experiment started in clean air at 15% RH. The corrosion rate was below the detection limit until the relative humidity was increased to 70%. The corrosion rate stabilized at about 0.01 nm/day after 4 days and did not change even though the relative humidity was increased to 80% RH. Formic acid did not have a dramatic effect on copper corrosion when present at concentrations from 10 to 220 ppb. When the formic acid concentration was increased to 460 ppb, the corrosion rate changed to 0.05 nm/day. It stayed at this level at 1000 ppb as well. An additional increase in the corrosion rate to 0.14 nm/day was recorded at the maximal formic acid concentration of 1590 ppb. The corrosion rate decreased gradually to low values when the formic acid concentration was lowered to 190, 80 and 0 ppb.

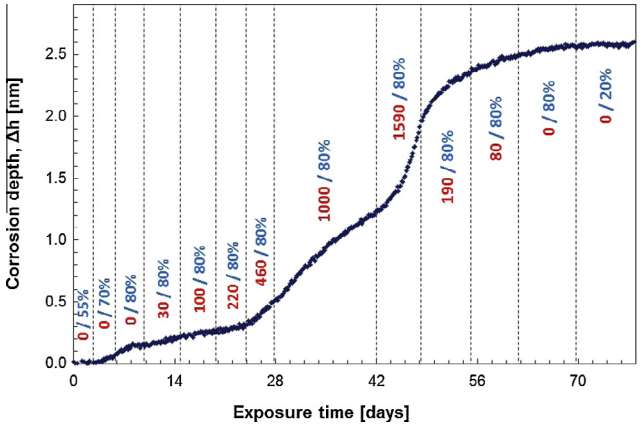

Fig. 5. Corrosion depth measured in air containing formic acid using a Cu-500 nm sensor; numbers give concentration of formic acid in ppb and relative humidity in per cent.

Cu-85 nm sensors were used in a similar experiment with a lower maximal relative humidity of 60%. Corrosion rates extracted from stabilized parts of the corrosion depth vs. time records are given in Table 2. Analogously to the previous experiment at 80% RH, the corrosion rate of copper only increased above about 0.01 nm/day when the concentration of formic acid was raised from 210 ppb to 420 ppb. Indeed, the increase was stronger under the wetter conditions. Whereas the corrosion rate continued to increase in more contaminated air at 80% RH, it remained nearly constant at 0.04 ± 0.01 nm/day at 60% RH until the formic acid concentration was raised to 2880 ppb.

4.1.3. Iron

Records for three iron Fe-800 nm sensors exposed to air with increasing concentrations of formic acid at 80% RH are plotted in Fig. 6. Sensors 2 and 3 were passive until the concentration of formic acid reached 1590 ppb when the corrosion depth increased dramatically. In five days, 190 nm of the iron track corroded on sensor 2. In half that time, 2.5 days, 11 nm corroded from sensor 3. After reducing the concentration of formic acid from 1590 to 190 ppb, the corrosion rate dropped rapidly and only an additional 8 nm of sensor 2 and 1 nm of sensor 3 corroded by the end of the experiment. Sensor 1 behaved somewhat differently: just under 3 nm of the iron track corroded in the first 28 days at formic acid concentrations up to 460 ppb and 80% RH. The sensor started to corrode rapidly when air with 1000 ppb of formic acid was fed into the chamber and 92 nm of iron corroded in this period of 14 days. A further increase in the pollutant concentration up to 1590 ppb

Table 2
Corrosion rate of copper sensors after stabilisation in the presence of formic acid.

c(HCOOH) (ppb)	Corrosion rate, v_{corr} (nm/day)	
	60% RH	80% RH
0	0.014 ± 0.003	0.010 ± 0.005
30–60	0.013 ± 0.003	0.013 ± 0.002
80–100	0.013 ± 0.002	0.009 ± 0.003
210–220	0.015 ± 0.003	0.012 ± 0.001
420–460	0.050 ± 0.014	0.053 ± 0.003
1000–1180	0.047 ± 0.011	0.051 ± 0.002
1550–1590	0.034 ± 0.005	0.143 ± 0.002
2880	0.043 ± 0.003	–

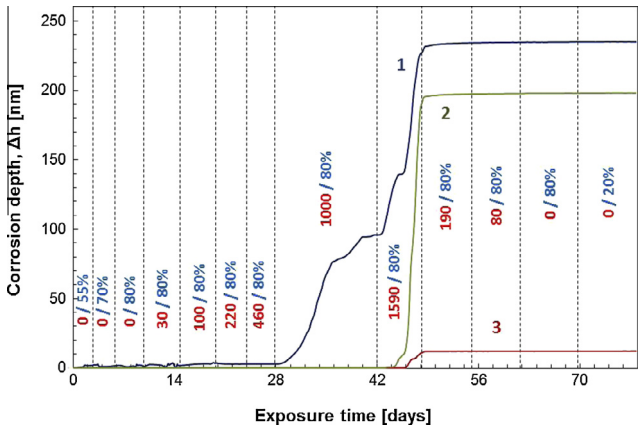

Fig. 6. Corrosion depth measured in air containing formic acid using three parallel Fe-800 nm sensors (1, 2, 3); numbers give concentration of formic acid in ppb and the relative humidity in per cent.

caused an increase in the corrosion rate and 130 nm of iron corroded in 6 days. At the end of the experiment, when the air aggressiveness was decreased, an additional 10 nm of iron corroded in 28 days.

The iron was initially in a passive state characterised by a negligible corrosion rate even at high RH. The passive layer failed when the formic acid concentration reached a critical concentration of 1000–1590 ppb. Activation of the surface was accompanied by localized corrosion in the form of thread-like red rust features that spread progressively over most of the surface. Even so, small areas without visible corrosion could be found at the end of the experiment. Such behaviour explains the large scatter in the measurements with the final corrosion depth of 148 ± 84 nm.

The behaviour of iron was clearly different from that of copper or bronze and from that of the silver and lead tested previously [19]. A concentration of at least 1000 ppb formic acid was needed to activate iron. The corrosion rate before activation was either nil or very low and irreproducible. The corrosion process progressed rapidly once the surface activated at a rate of up to 41 nm/day. When the formic acid concentration further decreased to 220, 100 and 0 ppb, the corrosion rates of previously-activated iron dropped to 0.10 ± 0.09, 0.04 ± 0.03 and 0.02 ± 0.02 nm/day, respectively. In experiments on other metals, the spread in measured corrosion depths was lower than ±20% [19]. Indeed, the technique requires corrosion to progress mainly uniformly to allow for calculation of corrosion depth from the ER record using Eq. (1). In any case, the sensors clearly responded to aggressive environments indicating that the technique has applications for corrosion monitoring even of non-uniformly corroding metals. It is also possible to pre-corrode a sensor to avoid the induction period.

4.2. Corrosivity limits for copper and bronze

A corrosivity classification for indoor atmospheres is defined in the ISO 11844-1 standard [14]. Based on the mass loss or mass gain of copper, silver, zinc and carbon steel coupons exposed for a year, atmospheric corrosivity can be split into five classes from IC 1 – Very low to IC 5 – Very high. This is practical since a threshold maximal corrosivity for a given exhibition room, showcase or storage facility, or for a given category of objects can be defined by conservators, management or authorities notwithstanding the type and quantity of pollutant present. The corrosivity classification based on air reactivity monitoring can thus be used to describe the quality of the atmosphere in general not just from the perspective of metallic materials [33].

The current measurements do not allow for the ISO 11844-1 classification due to several limitations. First and most important, the experiments were significantly shorter than the 1 year required by the standard. Because the mass gain or average corrosion depth of copper versus time curve usually has a parabolic shape [34], any linear extrapolation of short-term measurements can be misleading. Second, the response of the ER technique is close to the maximal depth of corrosion attack [19,23] whereas mass loss as assessed by the ISO 11844-1 standard corresponds to the mean corrosion depth. Third, the corrosion properties of thin metal films may differ from those of bulk metal. Fourth, a fresh sensor would need to be exposed to each set of conditions to avoid any effect due to corrosion films formed previously.

With the possible limitations in mind, the obtained corrosion rates in nm/day were compared to threshold limits for copper corrosivity classes calculated from mg/m^2/year of mass loss as described in the standard. Considering a constant corrosion rate, the upper threshold values for IC 1 and IC 2 are 0.015 and 0.060 nm/day. Fig. 7a shows the measured corrosion rates as a function of RH and formic acid concentration separated with iso-corrosion curves corresponding to the limits given above. The curves, which were calculated using the simplistic model of Eq. (2), must be regarded as only approximate due to the small number of measurements.

There is no corrosivity classification for alloy materials. However, the threshold limits defined in the previous paragraph for copper can be used for a rough estimation of the impact of the environment on α-bronze. Charts showing regions with identical corrosivity ranges as a function of the formic and acetic acid concentration and RH can then be constructed for bronze, see Fig. 7b and c. The corrosion rate of bronze in acetic acid at 55% RH and 310 ppb was below 0.015 nm/day, so the point is correctly shown as a triangle, although it falls above the iso-corrosion line.

Although bronze seemed to corrode more readily than copper in identical amounts of formic acid in these experiments, it must be stressed that the experiments were relatively short. Due to the

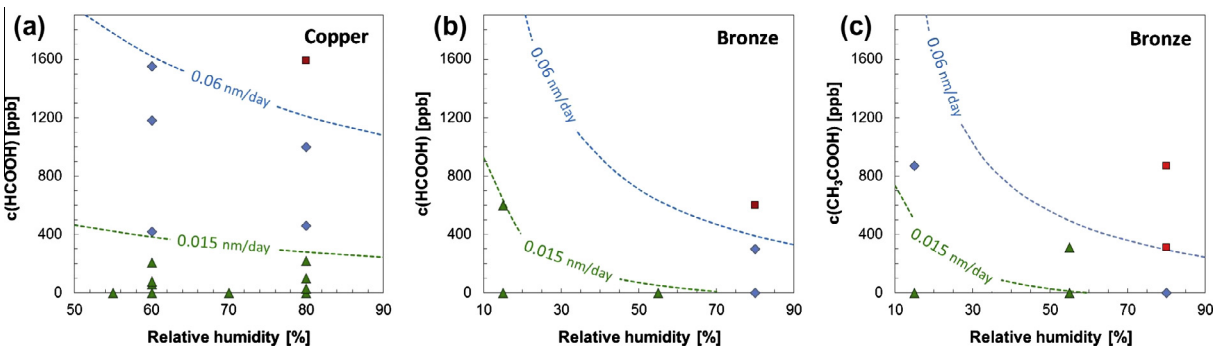

Fig. 7. Corrosion rates as a function of the relative humidity and carboxylic acid concentration; (a) copper and formic acid; (b) bronze and formic acid; and (c) bronze and acetic acid; experimental points: ▲$v_{corr} \leqslant 0.015$ nm/day, ♦ $0.015 < v_{corr} \leqslant 0.06$ nm/day, ■ $v_{corr} > 0.06$ nm/day; iso-corrosion curves are calculated from models (Eq. (2)).

formation of stable SnO_2, tin-bronze is usually somewhat more resistant to corrosion than copper in both aqueous and atmospheric exposure conditions [30,35,36]. Copper will dissolve preferentially from the α-phase bronze and the remaining tin will be incorporated into SnO_2 outdoors [36]. It may be that the corrosion reaction leading to a protective tin oxide patina is the one that was measured in these short experiments. Additional experiments will be needed to determine if the corrosion rate for bronze remains higher than that of copper.

Since rates of corrosion processes are affected by the presence of films of corrosion products, the experimental setup used here with changing air composition during experiments does not provide information on the corrosion rate of fresh pieces of metal as used for the ISO 11844-1 classification. The data in Fig. 7 may not be valid for such fresh surfaces, although it should be kept in mind that the exposure time required by the standard is a full year and it is doubtful that conditions within a real environment will be constant over that time. The goal of this work was to show that the corrosion rate changes with variations in climatic parameters even on previously-corroded surfaces and to assess the relative aggressiveness of the studied climates.

5. Conclusions

The effect of short-chain volatile carboxylic acids on the corrosion rate of copper and bronze was low up to the concentration of 200 ppb in air. Clear detrimental effects of the pollutants were observed when the concentration of formic or acetic acid reached about 300 ppb at an elevated relative humidity of 80% RH. The metals were little affected by the acids at relative humidities of up to 60%. The corrosion rates of both copper and bronze increased rapidly after the introduction of the pollutants, but decreased slowly for several days after their removal. The slow decrease was likely due to a low rate of desorption of the acids from the metal surfaces. The corrosion rate of bronze in the presence of formic acid was slightly higher than that of copper, at least for short time frames.

For iron, the critical concentration of formic acid in air at 80% RH leading to surface activation and rapid corrosion was found to be between 1000 and 1590 ppb.

The developed technology provided extreme sensitivity at the sub-nanometer level allowing for real-time corrosion monitoring in low-corrosivity indoor environments. Even small changes in air corrosivity caused a change in the measured corrosion rate within a short time.

Acknowledgments

This project has received funding from the European Union's Seventh Programme for research, technological development and demonstration under Grant agreement No. 226539. All members of the project team are thanked for their contributions. We wish to especially thank Bert Scheffel of Fraunhofer Institute for Electron Beam and Plasma Technology, Germany for designing the thin-film sensors and Yves Degres, Michel Jouannic and Patrice Le Garff from nke electronics, France for development of the electronic part and software.

References

[1] A.G. Allen, A.H. Miguel, Indoor organic and inorganic pollutants: in-situ formation and dry deposition in Southeastern Brazil, Atmos. Environ. 29 (1995) 3519–3526.
[2] P. Brimblecombe, The composition of museum atmospheres, Atmos. Environ. Part B 24 (1990) 1–8.
[3] L.T. Gibson, C.M. Watt, Acetic and formic acids emitted from wood samples and their effect on selected materials in museum environments, Corros. Sci. 52 (2010) 172–178.
[4] N.S. Baer, P.N. Banks, Indoor air pollution: effects on cultural and historic materials, Int. J. Museum Manage. Curatorship 4 (1985) 9–20.
[5] M. Ryhl-Svendsen, J. Glastrup, Acetic acid and formic acid concentrations in the museum environment measured by SPME-GC/MS, Atmos. Environ. 36 (2002) 3909–3916.
[6] E. Rocca, C. Rapin, F. Mirambet, Inhibition treatment of the corrosion of lead artefacts in atmospheric conditions and by acetic acid vapour: use of sodium decanoate, Corros. Sci. 46 (2004) 653–665.
[7] A. Schieweck, B. Lohrengel, N. Siwinski, C. Genning, T. Salthammer, Organic and inorganic pollutants in storage rooms of the lower Saxony State Museum Hanover, Germany, Atmos. Environ. 39 (2005) 6098–6108.
[8] G. Loupa, E. Charpantidou, E. Karageorgos, S. Rapsomanikis, The chemistry of gaseous acids in medieval churches in Cyprus, Atmos. Environ. 41 (2007) 9018–9029.
[9] American Society of Heating, Refrigeration and Air Conditioning Engineers (ASHRAE), Museums, Libraries, and Archives, Chapter 21 in Heating, Ventilating, and Air-Conditioning: Applications, Atlanta, ASHRAE, 2003.
[10] R. Reiss, P.B. Ryan, S.J. Tibbetts, P. Koutrakis, Measurement of organic acids, aldehydes, and ketones in residential environments and their relation to ozone, J. Air Waste Manage. Assoc. 45 (1995) 811–822.
[11] L.T. Gibson, B.G. Cooksey, D. Littlejohn, N.H. Tennent, A diffusion tube sampler for the determination of acetic acid and formic acid vapours in museum cabinets, Anal. Chim. Acta 341 (1997) 11–19.
[12] C. Chiavari, C. Martini, D. Prandstraller, A. Niklasson, L.-G. Johansson, J.-E. Svensson, A. Åslund, C.J. Bergsten, Atmospheric corrosion of historical organ pipes: the influence of environment and materials, Corros. Sci. 50 (2008) 2444–2455.
[13] L. Robinet, The role of organic pollutants in the alteration of historic soda silicate glass, PhD Thesis, University of Edinburg/Université de Paris VI, 2006, p. 39.
[14] ISO 11844-1, Corrosion of metals and alloys – classification of low corrosivity of indoor atmospheres – Part 1: determination and estimation of indoor corrosivity, International Organization of Standardization, Genève, Suisse, 2006.
[15] ANSI/ISA-71.04-1985, Environmental conditions for process measurement and control systems: Airborne contaminants, ANSI/ISA-The Instrumentation, System and Automation Society, 1986.
[16] E. Sacchi, C. Muller, Air quality monitoring at historic sites – redefining an environmental classification system for gaseous pollution, American Society of Heating, Refrigerating & Air-Conditioning Engineers, Inc., Atlanta GA, USA, 2005.
[17] Automated corrosion sensors as on-line real time process control tools (CORRLOG), Co-operative Research Project, 6th Framework Programme, Contract No. 018207, 09/2005–02/2008.
[18] Protection of cultural heritage by real-time corrosion monitoring (MUSECORR), Collaborative Project, 7th Framework Programme, Contract No. 226539, 06/2009–07/2012.
[19] T. Prosek, M. Kouril, M. Dubus, M. Taube, V. Hubert, B. Scheffel, Y. Degres, M. Jouannic, D. Thierry, Real-time monitoring of indoor air corrosivity in cultural heritage institutions with metallic electrical resistance sensors, Stud. Conserv. 58 (2013) 117–128.
[20] M. Kouril, T. Prosek, B. Scheffel, F. Dubois, High-sensitivity electrical resistance sensors for indoor corrosion monitoring, Corros. Eng. Sci. Technol 48 (4) (2013) 282–287. p. 48.
[21] M. Dubus, T. Prosek, Standardized assessment of cultural heritage environment by electrical resistance measurement, e-Preserv. Sci. 9 (2012) 67–71.
[22] T. Prosek, M. Kouril, L.R. Hilbert, Y. Degres, V. Blazek, D. Thierry, M.Ø. Hansen, Real time corrosion monitoring in the atmosphere using automated battery-driven corrosion loggers, Corros. Eng. Sci. Technol. 43 (2) (2008) 129–133.
[23] T. Prosek, N. Le Bozec, D. Thierry, Application of automated corrosion sensors for monitoring the rate of corrosion during accelerated corrosion tests, Mater. Corros. 65 (2014) 448–456.
[24] ASTM G96, Standard Guide for On-Line Monitoring of Corrosion in Plant Equipment (Electrical and Electrochemical Methods), West Conshohocken, USA: ASTM International.
[25] <www.institut-corrosion.fr> (assessed 07.05.14).
[26] H. Gil, C. Leygraf, Quantitative in situ analysis of initial atmospheric corrosion of copper induced by acetic acid, J. Electrochem. Soc. 154 (2007) C272–C278.
[27] H. Gil, C. Leygraf, Initial atmospheric corrosion of copper induced by carboxylic acids: a comparative in situ study, J. Electrochem. Soc. 154 (2007) C611–C617.
[28] H. Gil, C. Leygraf, J. Tidblad, GILDES model simulations of the atmospheric corrosion of copper induced by low concentrations of carboxylic acids, J. Electrochem. Soc. 158 (2011) C429–C438.
[29] P. Qiu, C. Leygraf, Multi-analysis of initial atmospheric corrosion of brass induced by carboxylic acids, J. Electrochem. Soc. 158 (2011) C172–C177.
[30] M.E. Warwick, Atmospheric corrosion of tin and tin alloys, International Tin Research Institute, Publication No. 602, 1980.
[31] J.M. Bastidas, M.P. Alonso, E.M. Mora, B. Chico, Corrosion of bronze by acetic and formic acid vapours, sulphur dioxide and sodium chloride particles, Mater. Corros. 46 (1995) 515–519.

[32] D.M. Bastidas, V.M. La Iglesia, Organic acid vapours and their effect on corrosion of copper: a review, Corros. Eng. Sci. Technol. 42 (2007) 272–280.
[33] J. Havermans, The Dutch Archival Act and harmonisation, Indoor Air Quality in Archives and Museums, Chalon-sur-Saône, April 21–23 2010, p. 37.
[34] C. Leygraf, T. Graedel, Atmospheric Corrosion, Wiley – Interscience, New York, 2000.
[35] M. Taube, A.H. King, W.T. Chase, Transformation of ancient Chinese and model two-phase bronze surfaces to smooth adherent patinas, Phase Trans. 81 (2008) 217–232.
[36] C.R. Southwell, C.W. Hummer, A.L. Alexander, Corrosion of metals in tropical environments, Part 7 – Copper and copper alloys – Sixteen Years' Exposure, NRL Report 6452, Naval Research Laboratory, Washington, D.C., 1966.